

## Nucleon-nucleon interaction with nonlocal tensor contribution for the ${}^3S_1$ - ${}^3D_1$ state

Mustafa M. Mustafa

*Faculty of Science (Sohag), Assiut University, Sohag, A.R. Egypt*

Elbadry S. Zahran

*Faculty of Science, Assiut University, Assiut, A.R. Egypt*

(Received 10 February 1988)

A nucleon-nucleon interaction for the  ${}^3S_1$ - ${}^3D_1$  state consisting of a local part plus a nonlocal separable tensor contribution of the form  $\lambda g(r)g(r')S_{12}$  is presented. The nonlocal part is repulsive and short ranged in agreement with the quark-exchange model. Ten potentials with ten different values of  $\lambda$  are considered.

### I. INTRODUCTION

There is an extensive interest in the literature in investigating the nucleon-nucleon interaction at small radii using the quark model, because it is believed that one gluon exchange between quarks plays the most important role in the nucleon-nucleon interaction.<sup>1</sup>

Cvetic *et al.*<sup>2</sup> argued that the interaction between clusters of quarks representing nucleons is expected to manifest itself in a nonrelativistic potential to a good approximation. Oka and Yazaki<sup>3</sup> claimed that the short-range repulsion of the nuclear force can be explained as a quark-exchange force with appropriate quark-quark interactions and that the quark-exchange force between two baryons is short-ranged and nonlocal.

A nonlocal potential model for the coupled  ${}^3S_1$ - ${}^3D_1$  state is presented here. It is the sum of a local and nonlocal part. The nonlocal contribution is both repulsive and of short range, in agreement with properties of the quark-exchange force.

The nonlocal potential of McKerrell *et al.*<sup>4</sup> also consists of a local and nonlocal part. The mixing between the  $S$  and  $D$  states in their model is partly carried out by adding a term of the form

$$\lambda_{uw}g(r) \int g(r')w(r')dr'$$

to the  $S$ -state radial equation and

$$\lambda_{uw}g(r) \int g(r')u(r')dr'$$

to the  $D$ -state radial equation, where  $u(r)$  and  $w(r)$  are the radial wave functions of the  $S$  and  $D$  states, respectively. These nonlocal terms are spin independent. The mixing between the two coupled states in the present

model is carried out by the tensor potential, avoiding the inconsistency of attributing spin-dependent properties to spinless quantities. The model of McKerrell *et al.*<sup>4</sup> would agree with our model if the relative strengths of the nonlocality parameters  $\lambda_u$ ,  $\lambda_w$ , and  $\lambda_{uw}$  of their model were constrained such that  $\lambda_u=0$  and  $\lambda_{uw}/\lambda_w = -\sqrt{2}$ .

### II. SITUATION OF THE EXPERIMENTAL PHASES

The  $\epsilon_1$  of the energy-dependent analysis of Arndt *et al.*<sup>5</sup> has a negative minimum in the low-energy range. The  $\epsilon_1$  of the recent analysis of Arndt *et al.*<sup>6</sup> has a positive minimum which is almost at the same energy as the old negative minimum of Arndt *et al.*<sup>5</sup>

The  ${}^3S_1$  and the  ${}^3D_1$  phases of the energy-dependent analysis of MacGregor *et al.*<sup>7</sup> are practically the same as those of Arndt *et al.*<sup>5,6</sup> The values of the  $\epsilon_1$  of this analysis are believed to be relatively small at low energies. A local potential of Reid's type<sup>8</sup> [see Eqs. (3.3)] is given as an example. This potential fits the scattering parameters of MacGregor *et al.*<sup>7</sup> to a very high degree of accuracy, (chi-squared/datum  $\simeq 10^{-3}$ ). Its binding energy, quadrupole moment, and  $D$ -state probability are  $-2.2237$  MeV,  $0.151$  fm<sup>2</sup>, and  $2.62\%$ , respectively. The small values of the quadrupole moment and the  $D$ -state probability are a direct consequence of the smallness of the  $\epsilon_1$  at low ener-

TABLE I. The values of the free parameters of the local potential with  $Q=0.151$  fm<sup>2</sup>.

$j$	$a_C^{(j)}$	$a_{CS}^{(j)}$	$a_T^{(j)}$
2	29 559 077 (-4)	20 128 682 (-5)	10 507 101 (-4)
3	-57 983 870 (-3)	-72 961 221 (-4)	-14 978 902 (-3)
4	35 786 100 (-2)	38 832 595 (-3)	82 785 484 (-3)
5	-87 576 714 (-2)	-71 641 255 (-3)	-17 710 272 (-2)
6	72 390 761 (-2)	40 119 935 (-3)	12 410 548 (-2)

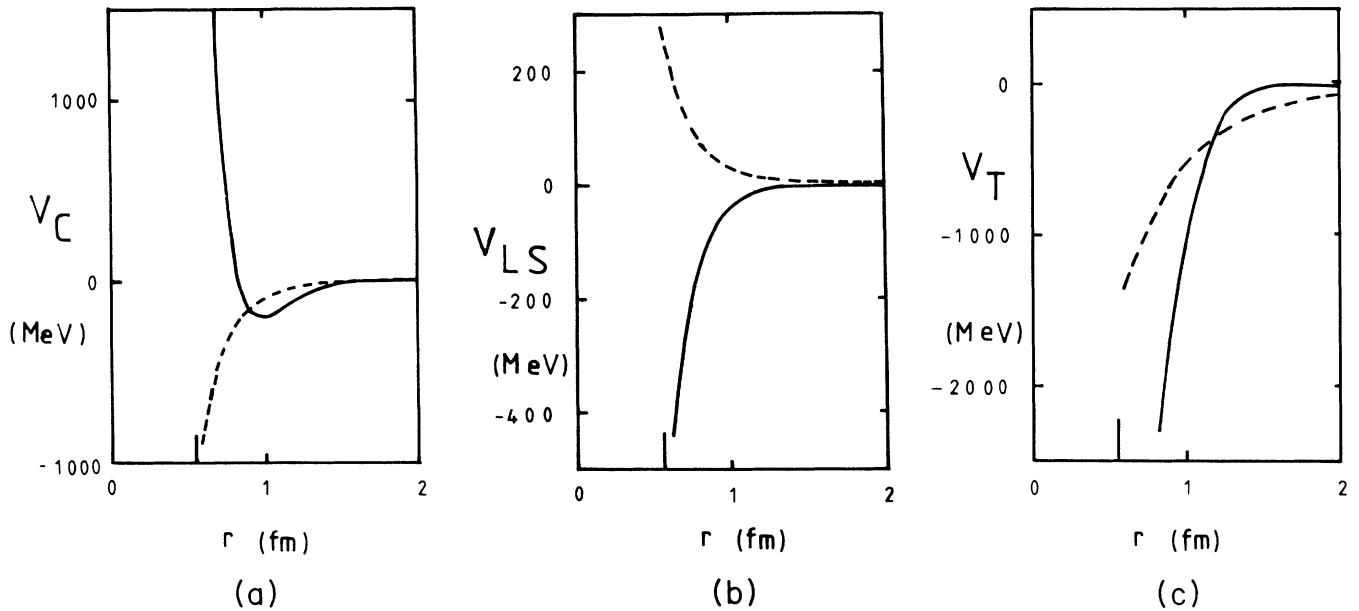


FIG. 1. The (a) central  $V_C$ , (b) spin-orbit  $V_{LS}$ , and (c) tensor  $V_T$  components of the local potential of Table I (solid lines) are compared to the Reid hard-core potential (dashed lines).

gies. The free parameters of this local potential are given in Table I. The radial dependencies of the potential and the deuteron wave functions are compared to the Reid hard-core (RHC) potential in Figs. 1 and 2, respectively.

The variations of  $\epsilon_1$  vs energy are shown in Fig. 3 for the three analyses and some realistic potential models.<sup>9-12</sup> The  $\epsilon_1$  of these models are more consistent with the  $\epsilon_1$  of MacGregor *et al.*<sup>7</sup> at low energies.

The situation of  $\epsilon_1$  at low energies is still unclear. Thus, the present potential model is chosen to be one that fits the experimental scattering parameters of MacGregor *et al.*<sup>7</sup>

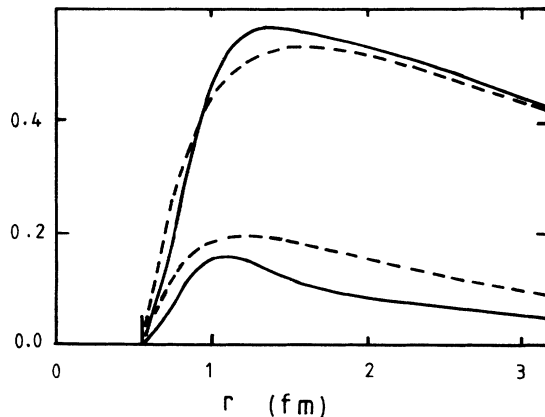


FIG. 2. The radial deuteron wave functions of the local potential of Table I (solid lines) are compared to the Reid hard-core potential (dashed lines). The upper (lower) curves are the  $u$  ( $w$ ) wave functions.

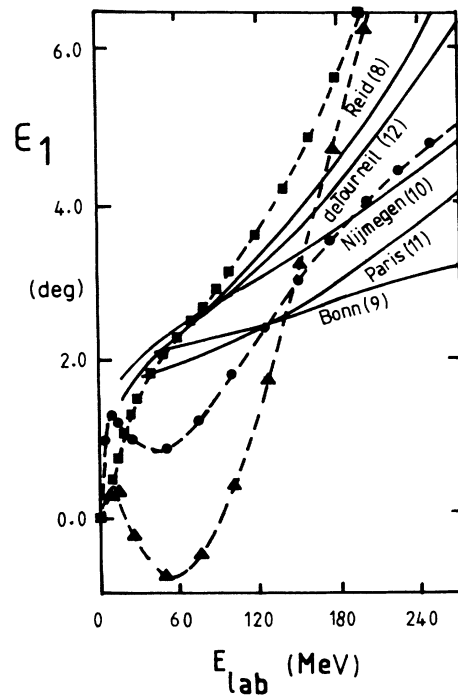


FIG. 3. The low-energy behavior of the  $\epsilon_1$  of MacGregor *et al.* (Ref. 7) (squares), Arndt *et al.* (Ref. 5) (triangles), Arndt *et al.* (Ref. 6) (circles), and some realistic potentials (Refs. 9-12). The references to the potentials are indicated on the corresponding graphs. Dashed lines have been drawn through experimental points. The line of the local potential of Table I is indistinguishable from the "experimental" line of MacGregor *et al.* (Ref. 7).

### III. THE NONLOCAL POTENTIAL MODEL

The nonlocal potential  $V$  has been assumed to be a sum of two parts, one is a separable nonlocal tensor potential  $V^N$  of the form

$$V^N = V_T^N S_{12} = \lambda g(r)g(r')S_{12} \quad (3.1)$$

with  $g(r) = e^{-\alpha r}$ ,  $\alpha = 2.1 \text{ fm}^{-1}$ , and the other part is a local potential  $V^L$  consisting of central ( $C$ ), spin-orbit ( $LS$ ), and local tensor ( $T$ ) contributions

$$V = V^L + V^N = V_C + V_{LS} \mathbf{L} \cdot \mathbf{S} + (V_T^L + V_T^N) S_{12} . \quad (3.2)$$

The choice of  $\alpha = 2.1 \text{ fm}^{-1}$  ensures the short range of the interaction.

The radial dependencies of  $V_C$ ,  $V_{LS}$ , and  $V_T^L$  are assumed to be as the following:

$$V_i = V_i^{\text{OPEP}} + \sum_{j=2}^n a_i^{(j)} r^{-1} e^{-j\mu r}, \quad i = C \text{ or } LS \quad (3.3a)$$

$$V_T^L = V_T^{\text{OPEP}} + A n^2 [1 + 3/(n\mu r) + 3/(n\mu r)^2] r^{-1} e^{-n\mu r} + \sum_{j=2}^n a_T^{(j)} r^{-1} e^{-j\mu r}, \quad (3.3b)$$

where

$$A = -14.94714 \text{ MeV}, \quad \mu = 0.7 \text{ fm}^{-1}, \quad n = 6,$$

$$V_C^{\text{OPEP}} = A r^{-1} e^{-\mu r},$$

$$V_{LS}^{\text{OPEP}} = 0,$$

and

$$V_T^{\text{OPEP}} = A [1 + 3/(\mu r) + 3/(\mu r)^2] r^{-1} e^{-\mu r}.$$

The second term in (3.3b) removes the  $r^{-2}$  and  $r^{-3}$  singularities of  $V_T^{\text{OPEP}}$ . It is not altogether necessary since a hard-core radius  $r_c = 0.54833 \text{ fm}$  is assumed. It is the same as that of the Reid hard-core potential to ease comparison with Reid's results.

The coupled radial Schrödinger equations in this case will have the following form:

$$u'' = (V_{SS} - k^2)u + V_{SD}w, \quad (3.4a)$$

$$w'' = V_{DS}u + (6/r^2 - k^2 + V_{DD})w, \quad (3.4b)$$

where

$$V_{SS} = V_C,$$

$$V_{SD} = V_{DS} = 2\sqrt{2}(V_T^L + V_T^N),$$

$$V_{DD} = V_C - 3V_{LS} - 2(V_T^L + V_T^N),$$

with the usual definition of the integral operator  $V_T^N$ .  $k^2$  is the energy in units of  $\text{fm}^{-2}$ . In the case of the deuteron,  $k^2 = -\gamma^2$ , where  $\gamma^2 \text{ fm}^{-2}$  is the binding energy.

### IV. THE NONLOCAL POTENTIALS WITH VARIOUS VALUES OF $\lambda$

Ten potentials with  $\lambda = 5, 25, 55, 80, 110, 140, 160, 200, 275,$  and  $375 \text{ fm}^{-3}$  have been produced by fitting the energy-dependent scattering parameters of MacGregor *et al.*<sup>7</sup> (0–260 MeV lab), the deuteron binding energy  $E_b$ , and the quadrupole moment  $Q$ , in a computer search scheme. The values of the free parameters of the potentials are listed in Table II.

#### A. The potential $\lambda 200$

The radial dependencies of the  $V_C$ ,  $V_{LS}$ , and  $V_T^L$  of the nonlocal potential  $\lambda 200$  (i.e., with  $\lambda = 200 \text{ fm}^{-3}$ ) are illustrated in Fig. 4, where they have been compared to the RHC potential. This particular potential has the relatively best fitting of the quadrupole moment  $Q = 0.283 \text{ fm}^2$  (Table III).

The deuteron wave functions are compared to those of the RHC potential in Fig. 5. The  $w$  wave has a small negative minimum ( $-0.0152$ ) just  $0.08 \text{ fm}$  outside the hard-core radius.

#### B. Potentials with

$\lambda = 5, 25, 55, 80, 110, 140, 160, 275,$  and  $375$

The simplest way to see that we have repulsion is that the binding energies of the local parts  $V^L$  ( $\lambda = 0$ ) are relatively large. It is seen from Table III that the values of the quadrupole moment  $Q$ , the  $D$ -state probability  $P_D$ , and the asymptotic  $D$ - to  $S$ -state ratio  $\eta$  increase as the short-ranged nonlocality become more repulsive. The deuteron wave functions for some of the values of  $\lambda$  are illustrated in Fig. 6.

The short-ranged nonlocal repulsion is obvious near the hard core (Fig. 6). An increase in  $\lambda$  leads to a decrease in the slope, and to an increasing shift of the maxima of the  $u$  and  $w$  wave functions towards larger radii (see also, Table IV).

A correlation may exist between the values of  $A_S$ ,  $r_d$ ,  $r_t$ , and  $a_t$  and, the sign of the deuteron wave functions just outside the hard core. This may be noticed in Tables III and IV. By increasing  $\lambda$ , the values of  $A_S$ ,  $r_d$ ,  $r_t$ , and  $a_t$  increase (Table III), except for the cases of  $\lambda = 5, 275,$  and  $375$  where there is a discontinuity in the pattern. The  $w$  wave function of the potential with  $\lambda = 5$  does not have a negative minimum and the  $u$  wave functions of the potentials with  $\lambda = 275$  and  $375$  have negative minima unlike the other members of Table IV.

The radial dependencies of the  $V_C$ ,  $V_{LS}$ , and  $V_T^L$  for the potentials with various values of  $\lambda$  are shown in Fig. 7. The cases of  $\lambda=55, 110, 160$  have not been drawn to avoid clutter. It is worthwhile to notice that as  $\lambda$  changes

(Fig. 7), an increasing attraction (repulsion) in the  $V_C$  potential would be partly compensated by an increasing repulsion (attraction) in both of the  $V_{LS}$  and the  $V_T^L$  potentials.

TABLE II. The values of the free parameters of the nonlocal potentials.

$\lambda$	$j$	$a_C^{(j)}$	$a_{LS}^{(j)}$	$a_T^{(j)}$
5	2	-07 217 334 (-8)	-15 726 902 (-6)	50 019 677 (-5)
	3	-46 886 128 (-6)	89 257 073 (-6)	-11 320 147 (-3)
	4	28 818 305 (-4)	0	82 006 231 (-3)
	5	-21 723 175 (-3)	-10 847 838 (-3)	-21 791 780 (-2)
	6	20 973 571 (-3)	25 563 484 (-3)	19 215 226 (-2)
	25	2	0	-15 726 902 (-6)
3		0	89 257 073 (-6)	-12 191 427 (-3)
4		0	0	82 006 231 (-3)
5		-31 707 218 (-4)	-21 156 642 (-4)	-21 791 780 (-2)
6		22 073 180 (-4)	59 703 691 (-4)	19 215 226 (-2)
55		2	0	-15 726 902 (-6)
	3	0	89 257 073 (-6)	-12 301 680 (-3)
	4	0	0	82 006 231 (-3)
	5	-76 820 768 (-4)	-23 031 527 (-5)	-21 791 780 (-2)
	6	11 702 495 (-3)	24 261 516 (-4)	19 215 226 (-2)
	80	2	0	-15 726 902 (-6)
3		-51 715 001 (-6)	89 257 073 (-6)	-12 409 688 (-3)
4		0	-10 607 215 (-4)	82 006 231 (-3)
5		-10 781 631 (-3)	73 377 707 (-4)	-21 799 093 (-2)
6		18 973 839 (-3)	-83 344 488 (-4)	19 215 226 (-2)
110		2	0	-15 726 902 (-6)
	3	0	89 257 073 (-6)	-12 624 104 (-3)
	4	0	0	82 006 231 (-3)
	5	-16 007 936 (-3)	31 870 508 (-4)	-21 791 780 (-2)
	6	30 164 618 (-3)	-43 415 531 (-4)	19 215 226 (-2)
	140	2	0	-15 726 902 (-6)
3		0	89 257 073 (-6)	-12 824 815 (-3)
4		0	0	82 006 231 (-3)
5		-20 085 143 (-3)	45 113 777 (-4)	-21 791 780 (-2)
6		39 632 616 (-3)	-70 124 008 (-4)	19 215 226 (-2)
160		2	0	-15 726 902 (-6)
	3	0	-89 257 073 (-6)	-12 959 939 (-3)
	4	0	0	82 006 231 (-3)
	5	-22 456 011 (-3)	54 640 591 (-4)	-21 791 780 (-2)
	6	45 325 346 (-3)	-89 440 457 (-4)	19 215 226 (-2)
	200	2	0	-15 726 902 (-6)
3		0	89 257 073 (-6)	-13 229 272 (-3)
4		0	0	82 006 231 (-3)
5		-26 932 262 (-3)	67 460 089 (-4)	-21 791 780 (-2)
6		56 280 723 (-3)	-11 546 276 (-3)	19 215 226 (-2)
275		2	0	-15 726 902 (-6)
	3	19 783 529 (-5)	89 257 073 (-6)	-13 154 455 (-3)
	4	11 070 086 (-3)	0	82 006 231 (-3)
	5	-96 907 690 (-3)	13 722 913 (-3)	-21 965 495 (-2)
	6	15 468 172 (-2)	-27 000 410 (-3)	19 215 226 (-2)
	375	2	0	-15 726 902 (-6)
3		15 543 613 (-4)	89 257 073 (-6)	-14 200 260 (-3)
4		0	0	82 062 231 (-3)
5		-69 599 718 (-3)	15 141 184 (-3)	-21 791 780 (-2)
6		13 761 023 (-2)	-29 544 909 (-3)	19 215 226 (-2)

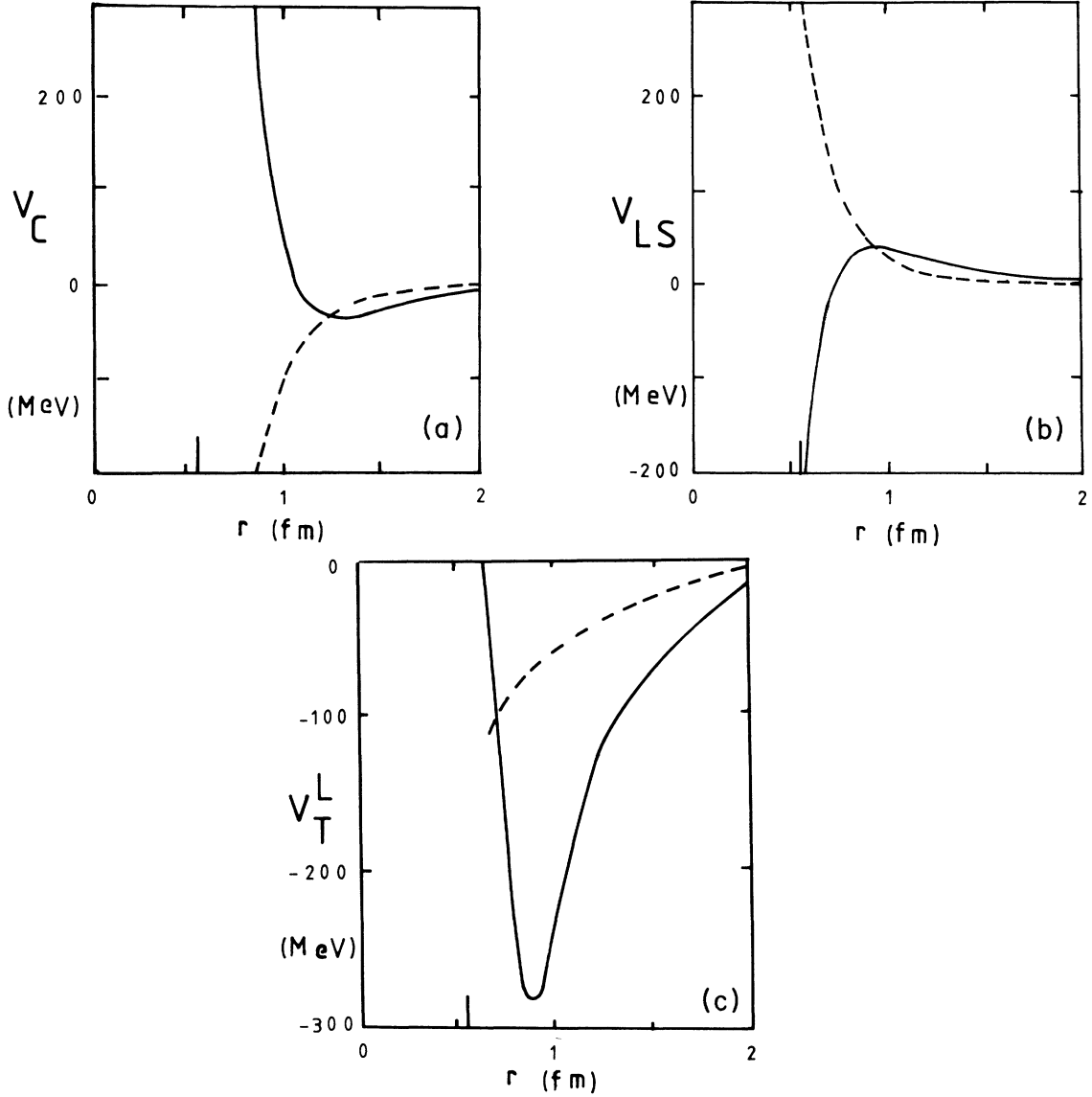


FIG. 4. The (a) central  $V_C$ , (b) spin-orbit  $V_{LS}$ , and (c) local tensor  $V_T^L$  components of the potential  $\lambda 200$  (solid lines) are compared to those of the Reid hard-core potential (dashed lines).

TABLE III. Deuteron properties and low-energy parameters of the nonlocal potentials. Experimental values are also listed.

$\lambda \text{ fm}^{-3}$	$E_b \text{ MeV}$	$E_b \text{ (MeV)}$ $\lambda=0$	$Q \text{ fm}^2$	$P_D \%$	$A_S \text{ fm}^{1/2}$	$\eta$	$r_d \text{ fm}$	$r_t \text{ fm}$	$a_t \text{ fm}$	$P$
5	-2.224 48	-3.136 14	0.239 53	4.9989	0.8861	0.021 98	1.968 80	1.7665	5.4274	-0.0147
25	-2.224 60	-7.500 07	0.259 23	6.0531	0.8815	0.023 26	1.962 79	1.7351	5.4045	-0.0119
55	-2.224 60	-17.052 66	0.264 08	6.2821	0.8851	0.023 46	1.971 05	1.7585	5.4220	-0.0126
80	-2.224 86	-26.041 34	0.266 81	6.4891	0.8876	0.023 49	1.976 63	1.7736	5.4334	-0.0131
110	-2.224 67	-37.772 86	0.272 18	6.7744	0.8894	0.023 75	1.981 76	1.7857	5.4427	-0.0130
140	-2.224 89	-49.394 76	0.275 84	6.9940	0.8913	0.023 86	1.986 40	1.7972	5.4516	-0.0126
160	-2.224 75	-57.054 52	0.278 55	7.1493	0.8923	0.023 97	1.989 20	1.8032	5.4568	-0.0132
200	-2.224 81	-71.991 03	0.282 97	7.3743	0.8945	0.024 11	1.994 59	1.8174	5.4683	-0.0133
275	-2.224 39	-91.892 42	0.295 87	8.3292	0.8853	0.025 54	1.981 63	1.7611	5.4267	-0.0132
375	-2.224 66	-124.4193	0.302 70	8.8181	0.8856	0.025 70	1.985 47	1.7660	5.4313	-0.0149
	-2.224 575		0.2859		0.8781	0.0271	1.953	1.759	5.424	
Exp.	$\pm 0.000 009$		$\pm 0.0003$		$\pm 0.0044$	$\pm 0.0008$	$\pm 0.003$	$\pm 0.005$	$\pm 0.004$	
	Ref. 13		Ref. 14		Ref. 15	Ref. 16	Ref. 17	Ref. 18	Ref. 18	

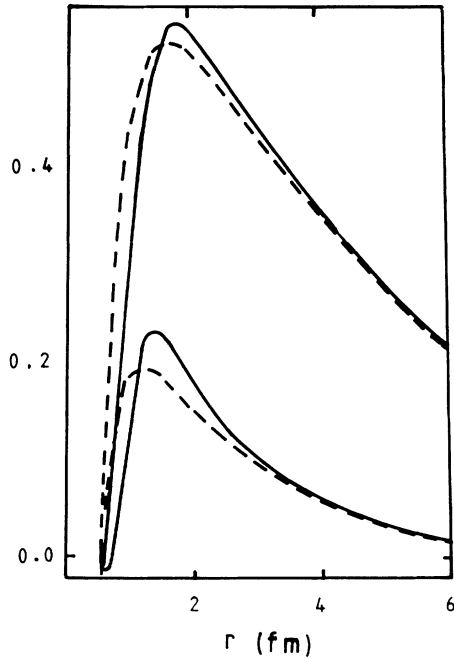


FIG. 5. The radial deuteron wave functions of the potential  $\lambda 200$  (solid lines) are compared to those of the Reid hard-core potential (dashed lines). The upper (lower) curves are the  $u$  ( $w$ ) wave functions.

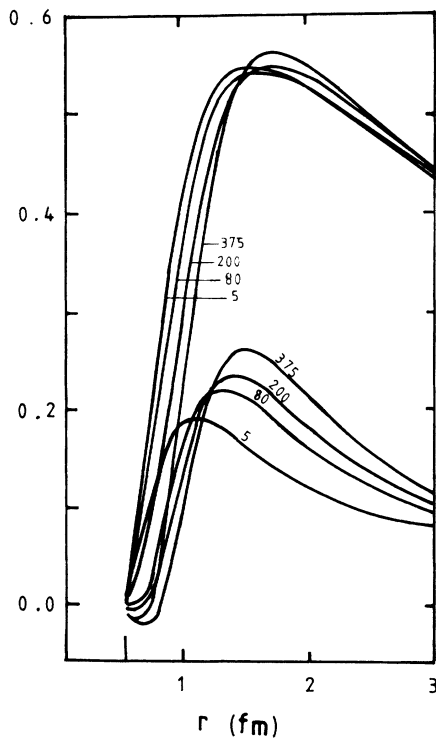


FIG. 6. The deuteron radial wave functions of the nonlocal potentials. The numbers on the graphs are the values of  $\lambda$ . The upper (lower) curves are the  $u$  ( $w$ ) wave functions. Not all wave functions are shown for clarity.

TABLE IV. The locations and the values of the maxima and minima of the radial deuteron wave functions of the nonlocal potentials.

$\lambda$ ( $\text{fm}^{-3}$ )	5	25	55	80	110	140	160	200	275	375
$u$ -wave max. at fm	0.545 35	0.539 78	0.540 51	0.541 29	0.542 75	0.544 06	0.544 77	0.546 17	0.556 01	0.559 50
$u$ -wave min. at fm	1.528 33	1.568 33	1.588 33	1.628 33	1.648 33	1.668 33	1.688 33	1.708 33	1.688 33	1.728 33
$w$ -wave max. at fm	0.0	0.0	0.0	0.0	0.0	0.0	0.0	0.0	-0.000 78	-0.006 26
$w$ -wave min. at fm	0.548 33	0.548 33	0.548 33	0.548 33	0.548 33	0.548 33	0.548 33	0.548 33	0.568 33	0.608 33
$u$ -wave max. at fm	0.190 62	0.207 64	0.211 30	0.215 90	0.220 02	0.223 96	0.226 67	0.230 57	0.249 44	0.257 42
$u$ -wave min. at fm	1.128 33	1.288 33	1.308 33	1.328 33	1.348 33	1.368 33	1.388 33	1.408 33	1.448 33	1.508 33
$w$ -wave max. at fm	0.0	-0.020 14	-0.015 51	-0.013 02	-0.012 16	-0.012 63	-0.013 30	-0.015 19	-0.015 26	-0.023 71
$w$ -wave min. at fm	0.548 33	0.628 33	0.628 33	0.628 33	0.628 33	0.628 33	0.628 33	0.628 33	0.648 33	0.668 33

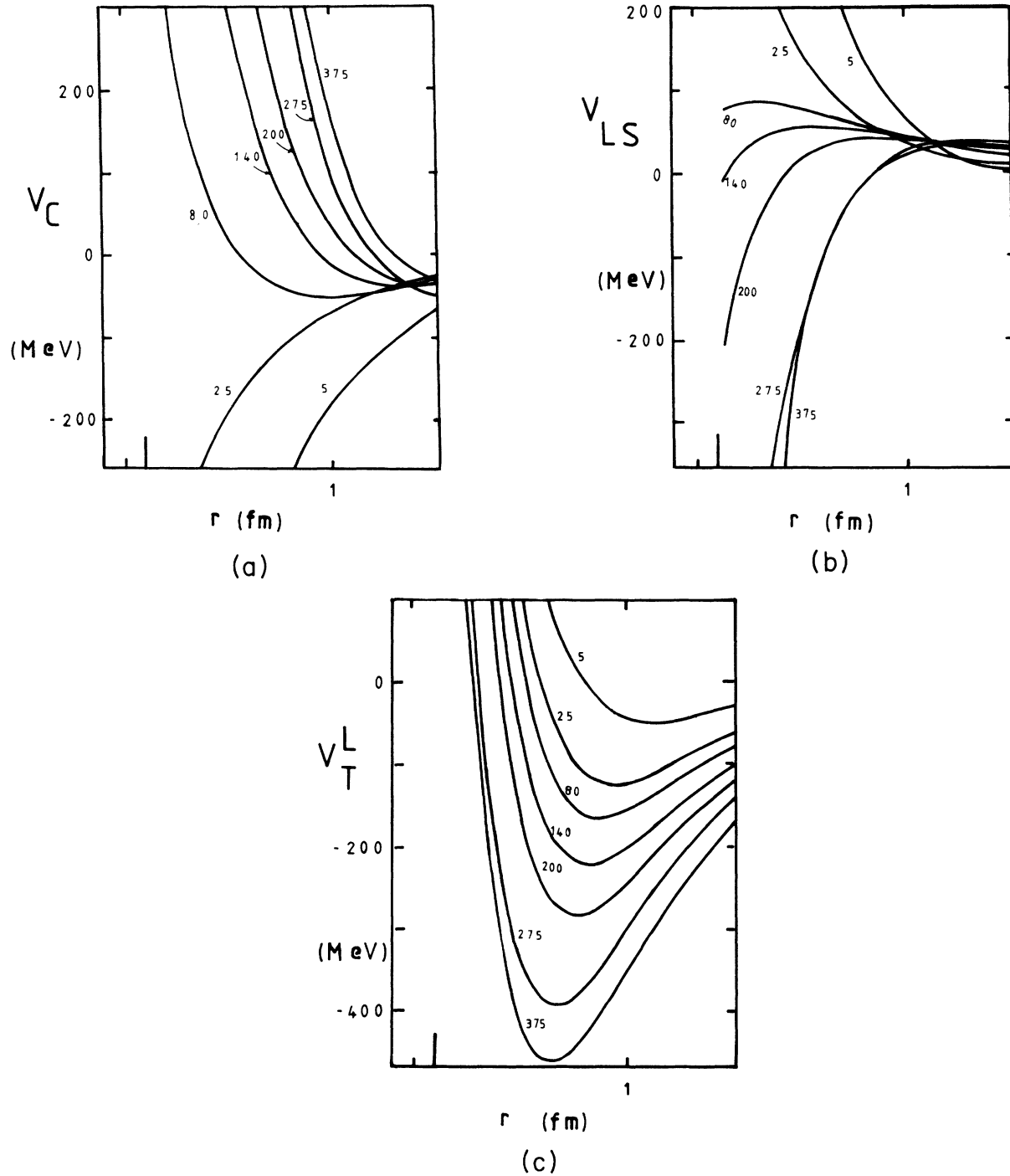


FIG. 7. The (a) central  $V_C$ , (b) spin-orbit  $V_{LS}$ , and (c) local tensor  $V_T^L$  components of the nonlocal potentials. The numbers on the graphs are the values of  $\lambda$ . The local components corresponding to  $\lambda = 55, 110, 160$  have not been shown for clarity.

## V. CONCLUSION

A simple nucleon-nucleon interaction incorporating a short-ranged repulsive nonlocality to take account of quark exchange is considered. The  $D$ -state probability  $P_D$ , the asymptotic  $D$ - to  $S$ -state ratio  $\eta$  and the quadrupole moment  $Q$  are sensitive to the nonlocality strength. They change uniformly with the strength of the repulsive

nonlocality.

The values of the asymptotic  $S$ -state amplitude  $A_S$ , the root-mean-square radius of the deuteron  $r_d$ , the triplet scattering length  $a_t$ , and the triplet effective range  $r_t$  are sensitive to the sign of the deuteron radial wave functions outside and close to the hard-core radius.

The experimental value of the quadrupole moment of the deuteron<sup>14</sup>  $Q_{\text{exp}} = 0.2859 \text{ fm}^2$  suggests that one value of  $\lambda$  ( $\lambda = 236.48 \text{ fm}^{-3}$ ) is best. When correcting for the

mesonic and relativistic effects ( $\Delta Q = 0.0063 \text{ fm}^2$ ),<sup>19</sup> the value of  $Q = Q_{\text{exp}} - \Delta Q = 0.2796 \text{ fm}^2$  suggests  $\lambda = 168.80 \text{ fm}^{-3}$ .

It was difficult to fit simultaneously  $r_d$ ,  $A_S$ , and  $a_r$ . Such difficulty is also found for the standard nonrelativistic potential models of the deuteron.<sup>17</sup>

#### ACKNOWLEDGMENT

We gratefully thank Dr. Mark W. Kermode for reading the manuscript and suggesting numerous improvements.

<sup>1</sup>K. Shimizu, Phys. Lett. **148B**, 418 (1984).

<sup>2</sup>M. Cvetič, B. Golli, N. Mankoc-Borstnik, and M. Rosina, Nucl. Phys. **A395**, 349 (1983).

<sup>3</sup>M. Oka and K. Yazaki, Nucl. Phys. **A402**, 477 (1983).

<sup>4</sup>A. McKerrell, M. W. Kermode, and M. M. Mustafa, J. Phys. **G 3**, 1349 (1977).

<sup>5</sup>R. A. Arndt, R. H. Hackman, and L. D. Roper, Phys. Rev. **C 15**, 1002 (1977).

<sup>6</sup>R. A. Arndt, L. D. Roper, R. A. Bryan, R. B. Clark, B. J. Verwest, and P. Signell, Phys. Rev. **D 28**, 97 (1983).

<sup>7</sup>M. H. MacGregor, R. A. Arndt, and R. N. Wright, Phys. Rev. **182**, 1714 (1969).

<sup>8</sup>R. V. Reid, Ann. Phys. (N.Y.) **50**, 411 (1968).

<sup>9</sup>R. Machleidt, K. Holinde, and Ch. Elster, Phys. Rep. **149**, 1 (1987).

<sup>10</sup>M. M. Nagels, T. A. Rijken, and J. J. de Swart, Phys. Rev. **D 17**, 768 (1978).

<sup>11</sup>M. Lacombe, B. Loiseau, J. M. Richard, R. Vinh Mau, J. Cote, P. Pires, and R. de Tourreil, Phys. Rev. **C 12**, 861 (1980).

<sup>12</sup>R. de Tourreil, B. Rouben, and D. W. L. Sprung, Nucl. Phys. **A242**, 445 (1975).

<sup>13</sup>C. Van der Leun and C. Alderliesten, Nucl. Phys. **A380**, 261 (1982).

<sup>14</sup>D. M. Bishop and L. M. Cheung, Phys. Rev. **A 20**, 381 (1979).

<sup>15</sup>I. Borbely, W. Gruebler, V. König, P. A. Schmelzbach, and A. M. Mukhamedzhanov, Phys. Lett. **160B**, 17 (1985).

<sup>16</sup>T. E. O. Ericson and M. Rosa-Clot, Nucl. Phys. **A405**, 497 (1983).

<sup>17</sup>S. Klarsfeld, J. Martorell, J. A. Oteo, M. Nishimura, and D. W. L. Sprung, Nucl. Phys. **A456**, 373 (1986).

<sup>18</sup>O. Dumbrajs *et al.*, Nucl. Phys. **B216**, 277 (1983).

<sup>19</sup>M. Kohno, J. Phys. **G 9**, L85 (1983).